Identification of ApoA4 as a sphingosine 1-phosphate chaperone in ApoM- and albumin-deficient mice[S]

Hideru Obinata,[1,*] Andrew Kuo,[†] Yukata Wada,[*] Steven Swendeman,[†] Catherine H. Liu,[§]
Victoria A. Blaho,[**] Rieko Nagumo,[*] Kenichi Satoh,[††] Takashi Izumi,[*] and Timothy Hla[1,†]

Gunma University Graduate School of Medicine,* Maebashi, Gunma 371-8511, Japan; Vascular Biology
Program,[†] Boston Children's Hospital, Department of Surgery, Harvard Medical School, Boston, MA 02115;
Weill Cornell Medical College,[§] Cornell University, New York, NY 10065; Sanford Burnham Prebys Research
Institute,** San Diego, CA 92037; and Shiga University,[††] Hikone, Shiga 522-8522, Japan

ORCID IDs: 0000-0001-8499-2278 (V.A.B.); 0000-0001-8355-4065 (T.H.)

Abstract   HDL-bound ApoM and albumin are protein chaperones for the circulating bioactive lipid, sphingosine 1-phosphate (S1P); in this role, they support essential extracellular S1P signaling functions in the vascular and immune systems. We previously showed that ApoM- and albumin-bound S1P exhibit differences in receptor activation and biological functions. Whether the physiological functions of S1P require chaperones is not clear. We examined ApoM-deficient, albumin-deficient, and double-KO (DKO) mice for circulatory S1P and its biological functions. In albumin-deficient mice, ApoM was upregulated, thus enabling S1P functions in embryonic development and postnatal adult life. The *Apom:Alb* DKO mice reproduced, were viable, and exhibited largely normal vascular and immune functions, which suggested sufficient extracellular S1P signaling. However, *Apom:Alb* DKO mice had reduced levels (∼25%) of plasma S1P, suggesting that novel S1P chaperones exist to mediate S1P function. In this study, we report the identification of ApoA4 as a novel S1P binding protein. Recombinant ApoA4 bound to S1P, activated multiple S1P receptors, and promoted vascular endothelial barrier function, all reflective of its function as a S1P chaperone in the absence of ApoM and albumin.[JLR] We suggest that multiple S1P chaperones evolved to support complex and essential extracellular signaling functions of this lysolipid mediator in a redundant manner.—Obinata, H., A. Kuo, Y. Wada, S. Swendeman, C. H. Liu, V. A. Blaho, R. Nagumo, K. Satoh, T. Izumi, and T. Hla. **Identification of ApoA4 as a sphingosine 1-phosphate chaperone in ApoM- and albumin-deficient mice.** *J. Lipid Res.* 2019. 60: 1912–1921.

Supplementary key words   apolipoproteins • sphingosine 1-phosphate receptors • lysophospholipid • high density lipoprotein • lipid transport • apolipoprotein A4 • apolipoprotein M

Sphingosine 1-phosphate (S1P) is a versatile lipid mediator essential for vascular development and lymphocyte trafficking. Five subtypes of cell-surface S1P receptors, S1PR1–5, mediate pleiotropic actions of extracellular S1P in multiple organ systems of vertebrates (1).

In contrast to eicosanoid lipid mediators, which are produced upon stimulation and act transiently, S1P circulates tonically in blood and lymph at high (0.1–1 μM) concentrations, which are significantly higher than the nanomolar concentrations required to activate S1P receptors. S1P in blood is produced primarily by red blood cells (RBCs) (2) and endothelial cells (3) and is secreted by specific S1P transporters, Mfsd2b (4) and Spns2 (5, 6), respectively. Due to its hydrophobic nature, S1P is poorly water soluble and requires carrier proteins for efficient transport and circulation. Most of plasma S1P (∼65%) is carried by HDL and the remainder by albumin (7). We have identified HDL-bound ApoM as a specific and physiologically relevant S1P chaperone (8), which is defined as a S1P carrier protein that facilitates specific receptor activation and biological responses.

Structurally, ApoM belongs to the lipocalin family of proteins and accommodates S1P in an eight-stranded antiparallel β barrel structure. Most of the ApoM in plasma is anchored to HDL by its retained hydrophobic N-terminal signal peptide (9). Although ApoM is found only in 5% of total HDL particles, this subpopulation of HDL accounts for almost all of the lipoprotein-associated S1P (8). HDL-bound S1P is important in vascular barrier function (8, 10),

bone marrow lymphopoiesis (11), liver function (12) and regeneration (13), restraint of inflammatory responses (14), brown adipocyte development (15), and control of blood pressure via NO release (16).

Interestingly, ApoM- and albumin-bound S1P show functional differences with respect to S1P signaling. Both ApoM- and albumin-S1P increase the barrier function of endothelial cells, but ApoM-S1P shows more sustained effects (16, 17). Suppression of endothelial inflammatory responses (14) and regulation of lymphopoiesis (11) are observed only in ApoM-S1P. Considering that albumin is able to bind many hydrophobic molecules in a promiscuous manner, ApoM serves as a specific S1P chaperone that protects and transfers S1P to its receptors so that efficient signaling can take place. In addition, ApoM-bound S1P is more stable than albumin-bound S1P in vivo (3, 18). However, albumin is able to compensate for the functions of ApoM to some extent. Although ApoM-deficient mice show various functional defects, such as increased vascular permeability (8, 10) and dysregulated lymphopoiesis (11), they still retain 40% of plasma S1P in the albumin fraction (8), which is sufficient to support the essential functions of S1P, such as embryonic vascular development and lymphocyte trafficking. In contrast, sphingosine kinase 1/2 deficiency, which results in no S1P production, leads to embryonic lethality due to vascular developmental defects (19). Adult plasma S1P-less mice derived from postnatal deletion of the *Sphk1* and *Sphk2* genes, show profound lymphopenia due to deficient lymphocyte egress from lymphoid organs (2).

In this study, we studied ApoM- and albumin-deficient mice to determine the compensatory functions of the two S1P chaperones. We also crossed ApoM-deficient mice with albumin-deficient mice to examine the functional consequences from the loss of the two major S1P carrier proteins. Double-null mice were still viable and retained 25% of plasma S1P, which suggested the existence of the additional S1P carrier protein(s). By protein fractionation of the double-null plasma followed by the shot-gun proteomic analysis, we identified ApoA4 as a novel S1P carrier protein. ApoA4 showed a S1P-binding property comparable to albumin, and ApoA4-bound S1P activated S1P receptors efficiently.

MATERIALS AND METHODS

Animals

All animal protocols were approved by the Institutional Animal Care and Use Committee of the Boston Children's Hospital and Weill Cornell Medical College. ApoM-deficient mice in the C57BL/6 background were described previously (8, 20). Albumin-deficient mice (B6;129S5-*Alb^{tm1Lex}*/Mmucd) were obtained from Mutant Mouse Regional Resource Centers (RRID: MMRRC_032140-UCD) and backcrossed at least seven times with C57BL/6 mice before crossing with the ApoM-deficient mice. Double heterozygotes in the *Alb* and *Apom* alleles were intercrossed to prepare the double-null homozygotes. Whole blood and serum specimens from the mice were subjected to laboratory tests for blood biochemistry (liver and renal panels) and blood cell counts in the

Laboratory of Comparative Pathology, Memorial Sloan-Kettering Cancer Center, New York, NY.

Chromatography

FPLC analyses were performed using an ÄKTApurifier FPLC system (GE Healthcare Life Sciences). Plasma samples were separated by size exclusion chromatography with tandemly connected Superose™ 6 and Superdex™ 200 columns (16 × 600 mm each) at the flow rate of 0.5 ml/min using PBS containing 1 mM EDTA as the running solvent. Optical absorbance at 280 nm was monitored for protein concentrations, and the cholesterol concentration was determined by LabAssay™ cholesterol kit according to the manufacturer's instructions (FUJIFILM Wako Pure Chemical Corp.). RESOURCE Q columns (1 ml; GE Healthcare Life Sciences) were used for anion exchange chromatography at the flow rate of 4 ml/min with a NaCl gradient from 0 to 500 mM in 5 min in the running solvent (20 mM Tris-HCl, pH 8.0).

S1P measurements

S1P was quantified by LC-MS/MS analysis using a LCMS-8050 system (triple quadrupole; Shimadzu) as described (21). Deuterated-S1P (S1P-d7 from Avanti Polar Lipids) was used as an internal standard. The *m/z* transitions for the selected reaction monitoring of S1P and S1P-d7 were *m/z* 380.0–264.0 and *m/z* 387.0–271.0, respectively.

Protein identification by nano LC-MS/MS analysis

Protein samples from the plasma fractions were separated by SDS-PAGE with a 4–12% precast gel (Bolt™ 4–12% Bis-Tris Plus Gels; Thermo Fisher Scientific). The gel was cut into several pieces, dehydrated by acetonitrile, and dried under vacuum. The proteins contained in the gel pieces were reduced by DTT and alkylated by iodoacetamide, and digested overnight with Trypsin/Lys-C Mix (Promega). Trypsin and Lys-C digest the C-terminal side of lysine (trypsin and Lys-C) and arginine (trypsin). The digests were then extracted in acetonitrile with 1% formic acid and subjected to analysis by a NanoFrontier eLD coupled with a nano flow HPLC system (Hitachi High-Technologies) as described (22). Raw data were converted into peaklist files (.mgf) using NanoFrontier eLD data processing software (version 2008) and subjected to a search against SwissProt mouse sequences (February 2016, 16,772 entries) using Mascot search algorithm (Matrix Science, version 2.4.0). Searches were performed with a mass measurement tolerance of 0.2 Da for both precursor and fragment ions. A maximum of one missed cleavage was allowed. Carbamidomethylation of cysteine residues and oxidation of methionine, tryptophan, and histidine residues were searched as fixed and variable modifications, respectively. The ion score significance threshold was chosen to be 0.05.

Recombinant protein expression and analyses

Histidine-tagged recombinant proteins for human afamin (AFM), vitamin D binding protein (DBP), α-fetoprotein (aFP), and albumin were expressed in HEK cells and recovered in culture supernatants. Histidine-tagged ApoA4 and ApoM were expressed in an *Escherichia coli* BL-21 strain, and recovered in the soluble fractions of the cell lysate. These recombinant proteins were purified by using a HisTrap FF column (5 ml; GE Healthcare Life Sciences) with a linear gradient of imidazole from 20 to 500 mM, then dialyzed against PBS using Slide-A-Lyzer™ dialysis cassettes (Thermo Fisher Scientific).

S1P binding assay

S1P (1 μM) was incubated with one of the recombinant proteins for 24 h at 4°C. Free S1P was removed by using Zeba™ Spin

desalting columns (0.5 ml; Thermo Fisher Scientific). The protein-bound S1P was extracted in methanol, and the S1P concentrations were determined by LC-MS/MS analysis as described above.

Western blot analysis

Protein samples were separated by SDS-PAGE with a 4–12% precast gel (Bolt™ 4–12% Bis-Tris Plus Gels), then transferred onto PVDF membranes by using an iBlot 2 dry blotting system (Thermo Fisher Scientific) according to the manufacturer's instructions. The PVDF membranes were blocked with 5% skim milk in TBS containing 0.1% Tween20 (TBS-T, pH 7.6), then incubated with primary antibodies diluted in the blocking solution at 4°C overnight. After washing with TBS-T three times, the membranes were incubated with HRP-conjugated secondary antibodies in the blocking solution for 1 h at room temperature. The signals were visualized by using Luminata Forte Western HRP substrate reagent (Millipore) according to the manufacturer's instructions, and recorded by using an ImageQuant LAS 4010 image analyzer system (GE Healthcare). Primary antibodies used in this study were anti-ApoM (Abcam #EPR2904, 1:2,500), anti-ApoA4 (Cell Signaling Technology #5700 for human ApoA4 or R&D Systems #AF8125-SP for mouse ApoA4, 1:2,500), anti-Akt (Cell Signaling Technology #4060, 1:5,000), anti-phospho Akt (Cell Signaling Technology #9271, 1:5,000), anti-ERK1/2 (Cell Signaling Technology #9102, 1:10,000), and anti-phospho ERK1/2 (Cell Signaling Technology #9106, 1:10,000).

Cell culture

Human umbilical vein endothelial cells (HUVECs) were cultured on human-fibronectin coated dishes using M199 medium (Corning) supplemented with 10% fetal bovine serum (VWR), endothelial cell growth factors from sheep brain extract, 5 U/ml heparin (Sigma), and 1% penicillin-streptomycin (Corning) in a 37°C incubator with 5% CO_2 (16).

Endothelial cell permeability assay

Barrier function of HUVECs was assayed by measuring the impedance of a cell-covered electrode by an electric cell-substrate impedance sensing instrument Zθ device (ECIS; Applied BioPhysics) in accordance with the manufacturer's instructions. In brief, a 96-well electrode array (96W10idf) was precleaned with 10 mM L-cysteine for 15 min at room temperature, washed with sterile water, coated with fibronectin for 30 min at 37°C, and incubated with complete M199 medium for electrical stabilization. HUVECs (passages 4–7) were seeded at a density of 2.5×10^4 cells/well and cultured to confluence. Cells were starved for 2–3 h with serum- and growth factor-free M199 medium. Electric resistance was collected at single frequency for 30 min to obtain baseline resistance. Next, HUVECs were treated with 100 nM of BSA, ApoM-Fc, or recombinant ApoA4 preincubated with or without S1P. Resistance was expressed as fractional resistance, normalizing to the baseline at time 0.

Statistical analyses

Results are expressed as mean ± SD. Sample sizes are indicated in the figure legends. Statistical analysis was performed using R software (version 3.6.0), a language and environment for statistical computing and graphics (https://www.r-project.org). A Chi-square goodness of fit test was performed to examine whether the birthrate of mice with each genotype followed the Mendelian ratio (Fig. 1A). A multiple linear regression model was applied to examine the statistical differences of the growth curves between four genotype groups (Fig. 1B). Student's *t*-test was used for comparing parametric variables between two groups. One-way ANOVA was performed for comparing more than two groups, followed by the post hoc Tukey-Kramer's multiple comparison test. Statistical significance was defined as $P < 0.05$.

RESULTS

To assess the requirement for the two major S1P chaperones, albumin and ApoM, we intercrossed $Alb^{+/-}/Apom^{+/-}$ double-heterozygous mice. As shown in **Fig. 1A**, the offspring contained viable mice with all possible genotypes following the Mendelian ratio. ApoM deficiency [both in ApoM KO and double-KO (DKO) mice] resulted in the smaller body size, especially in female mice (Fig. 1B, supplemental Fig. S1), which is in accordance with the previous report (15). However, both male and female DKO mice did not exhibit discernible abnormalities in behavior and appeared healthy. Blood biochemistry (liver and renal panel) revealed that total protein and creatinine are significantly lower in DKO mice compared with WT mice, while alkaline phosphatase and cholesterol were higher in DKO mice (**Table 1**). Blood cell count analyses showed that RBCs in DKO mice showed a minor size difference, indicated by the lower values in mean corpuscular volume (volume) and mean corpuscular hemoglobin (hemoglobin content) and the higher value in red cell distribution width-coefficient of variation (coefficient of variation in size distribution). The white blood cell count in DKO mice was almost doubled, mainly due to the increase in lymphocyte count, which is consistent with our previous findings in *Apom* KO mice that showed enhanced bone marrow lymphopoiesis and lymphocytosis (11). These results suggest that these two S1P chaperones are not indispensable for mouse embryonic development and immune cell trafficking.

Neither albumin nor ApoM can be detected in the plasma from the double-null homozygotes in *Alb* and *Apom* genes (**Fig. 2A**), and plasma albumin levels did not change significantly in *Apom* KO plasma (Fig. 2B). However, plasma ApoM levels were significantly increased in *Alb* KO plasma (Fig. 2C), suggesting a compensatory increase of this S1P chaperone.

Next, we measured S1P concentrations in plasma from the mice with each genotype (**Fig. 3**). ApoM deficiency resulted in ∼60% decrease in the plasma S1P concentration (from 445 to 170 nM), which is consistent with the previous results (8). On the other hand, albumin deficiency led to only 17% decrease (not statistically significant), though albumin is bound to ∼30% of S1P in plasma (7). This could be partly explained by the fact that ApoM protein level is upregulated in the albumin-deficient mice (see above). In DKO mouse plasma, S1P was decreased by ∼73% (from 445 to 119 nM). Considering that DKO mice are viable without severe abnormalities, the remaining 27% of S1P is sufficient to maintain vital S1P-S1P receptor signaling functions.

To elucidate the plasma S1P distribution in lipoprotein and lipoprotein-free fractions, we fractionated the plasma by size exclusion chromatography (**Fig. 4**). In WT plasma, most of the S1P was found in HDL fractions and the rest found in lipoprotein-free protein (LPFP) fractions

A

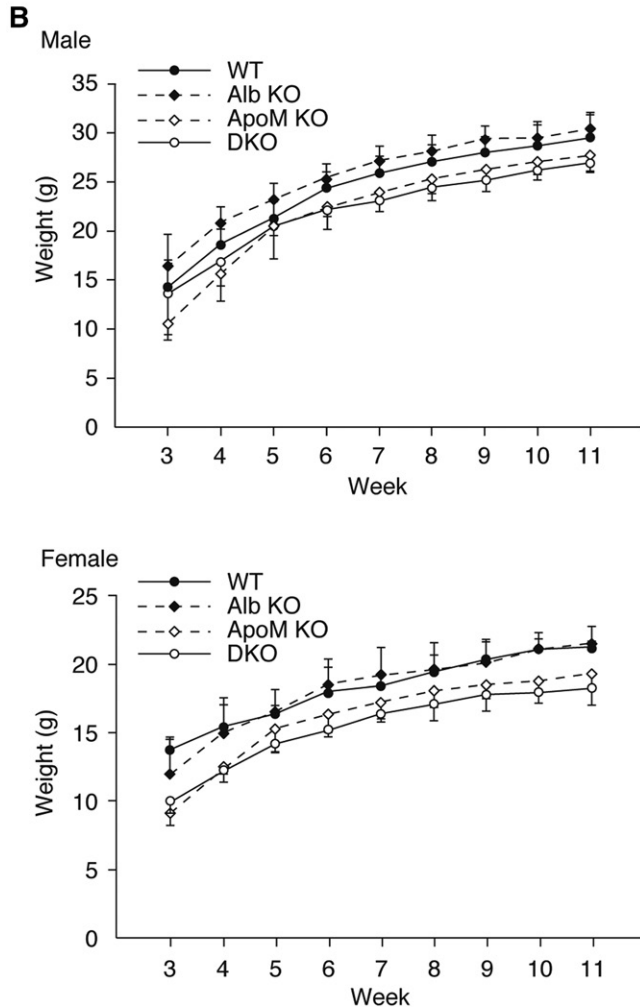|	*apom* allele		
alb allele	+/+	+/−	−/−
+/+	8	20	9
+/−	36	55	36
−/−	12	31	9

B

Male

Female

Fig. 1. ApoM KO, Alb KO, and DKO mice. A: $Alb^{+/-}/Apom^{+/-}$ double-heterozygous mice were intercrossed. The number of the pups with each genotype are shown, which are not significantly different from the Mendelian ratio ($P = 0.086$ in Chi-square goodness of fit test). B: Body weights of the mice under normal chow were recorded every week after weaning (at 3 week) until they were 11 weeks old. Data are shown as mean ± SD (n = 4–8). A multiple linear regression model was applied to examine the statistical differences of the growth curves between the four groups (supplemental Fig. S1). Significant differences ($P < 0.05$) were observed in WT versus Alb KO, WT versus ApoM KO, and WT versus DKO in the male group and in WT versus ApoM KO and WT versus DKO in the female group.

TABLE 1. Blood biochemistry and blood cell count

	WT	DKO
Blood biochemistry		
(liver/renal panel)		
BUN (mg/dl)	34.5 ± 4.8	30.3 ± 2.5
CREA (mg/dl)[a]	**0.23 ± 0.03**	**0.17 ± 0.02**
BUN/CREA ratio	155.6 ± 31.8	179.6 ± 19.3
ALP (U/l)[b]	**73.3 ± 8.1**	**127.3 ± 24.7**
ALT (U/l)	52.5 ± 17.9	46.0 ± 8.1
AST (U/l)	68.3 ± 24.1	53.3 ± 5.5
GGT (U/l)	0	0
TBIL (mg/dl)	0.2 ± 0.0	0.1 ± 0.0
DBIL (mg/dl)	0	0
IBIL (mg/dl)	0.2 ± 0.0	0.1 ± 0.0
TP (g/dl)[b]	**5.2 ± 0.2**	**3.9 ± 0.2**
GLOB (g/dl)[b]	**2.3 ± 0.1**	**2.8 ± 0.2**
P (mg/dl)	9.4 ± 1.1	9.1 ± 0.6
Ca (mg/dl)	10.1 ± 0.9	9.3 ± 0.5
GLU (mg/dl)	273.0 ± 113.5	202.5 ± 29.6
CHOL (mg/dl)[b]	**90.3 ± 10.8**	**145.5 ± 10.2**
TRIG (mg/dl)	155.8 ± 53.9	131.8 ± 47.7
CK (U/l)	197.3 ± 111.3	170.3 ± 214.5
TCO2 (mEq/l)	23.8 ± 6.7	23.5 ± 6.2
Na (mEq/l)	150.0 ± 2.8	150.3 ± 1.3
K (mEq/l)	8.9 ± 0.9	8.2 ± 1.1
Cl (mEq/l)	108.0 ± 2.2	108.0 ± 0.8
Na/K ratio	19.0 ± 2.2	18.5 ± 2.4
Anion gap	26.3 ± 3.3	27.3 ± 5.8
RBC and platelet indices		
RBC (M/ul)	10.1 ± 0.1	10.4 ± 0.2
HGB (g/dl)	14.9 ± 0.3	14.6 ± 0.3
HCT (%)	53.6 ± 0.5	52.3 ± 1.5
MCV (fl)[b]	**52.9 ± 0.6**	**50.2 ± 0.6**
MCH (pg)[b]	**14.7 ± 0.1**	**14.0 ± 0.1**
MCHC (g/dl)	27.7 ± 0.3	27.8 ± 0.4
RDW-SD (fl)	30.8 ± 0.4	31.1 ± 2.4
RDW-CV (%)[b]	**22.6 ± 0.2**	**24.1 ± 0.7**
RET number (K/ul)	409.7 ± 30.0	377.5 ± 35.6
RET (%)	4.1 ± 0.3	3.6 ± 0.3
PLT (K/ul)	722.8 ± 202.2	1013.3 ± 170.0
PDW (Fl)	6.5 ± 0.4	6.6 ± 0.7
MPV (Fl)	5.9 ± 0.4	5.8 ± 0.5
WBC counts		
WBC number (K/ul)[b]	**7.86 ± 2.39**	**13.89 ± 3.31**
NEUT# (K/ul)	1.51 ± 0.42	1.02 ± 0.19
LYMPH number (K/ul)[b]	**6.11 ± 2.65**	**12.48 ± 3.11**
MONO number (K/ul)	0.12 ± 0.06	0.15 ± 0.04
EO number (K/ul)	0.13 ± 0.07	0.23 ± 0.07

Whole blood and serum specimens from the mice were subjected to laboratory tests for blood biochemistry (liver and renal panels) and blood cell counts. Data represent mean ± SD (n = 4). Parameters significantly different are in boldface type. Note that a few of the minor statistically significant differences might be due to type I errors because multiple comparisons are performed. BUN, blood urea nitrogen; CREA, creatinine; ALP, alkaline phosphatase; ALT, alanine aminotransferase; AST, aspartate aminotransferase; GGT, γ-glutamyltranspeptidase; TBIL, total bilirubin; DBIL, direct bilirubin; IBIL, indirect bilirubin; TP, total protein; GLOB, globulin; P, phosphate; Ca, calcium; GLU, glucose; CHOL, cholesterol; TRIG, triglyceride; CK, creatine kinase; TCO2, total CO2; Na, sodium; K, potassium; Cl, chloride; HGB, hemoglobin; HCT, hematocrit; MCV, mean corpuscular volume; MCH, mean corpuscular hemoglobin; MCHC, mean corpuscular hemoglobin concentration; RDW-SD, red cell distribution width-SD; RDW-CV, red cell distribution width-coefficient of variation; RET, reticulocyte; PLT, platelet; PDW, platelet distribution width; MPV, mean platelet volume; WBC, white blood cell; NEUT, neutrophil; LYMPH, lymphocyte; MONO, monocyte; EO, eosinophil.
[a]$P < 0.05$, in Student's t-test.
[b]$P < 0.01$, in Student's t-test.

(protein-rich fractions that elute after lipoproteins) as reported previously (7, 8). In the *Apom* KO plasma, S1P was found exclusively in the LPFP fractions, whereas in the *Alb* KO plasma, all of the S1P was localized in the HDL fractions. This confirms that albumin and ApoM are two major carriers for S1P in plasma and that S1P chaperones can compensate for each other. In the absence of these two major carrier proteins, S1P was mainly found in the LPFP fractions of the DKO plasma, suggesting that additional
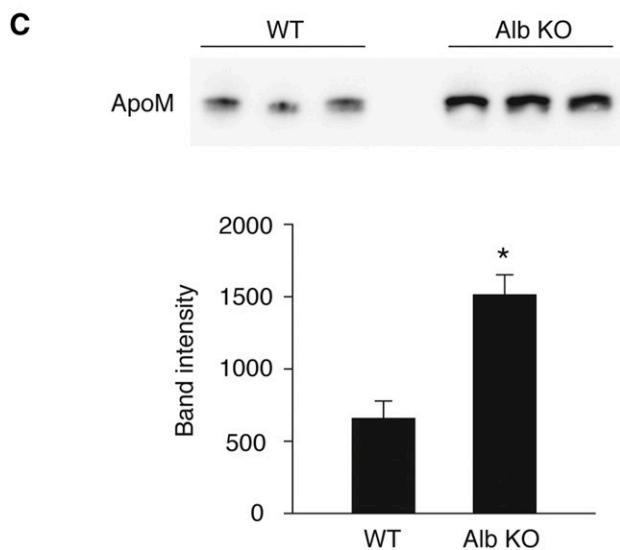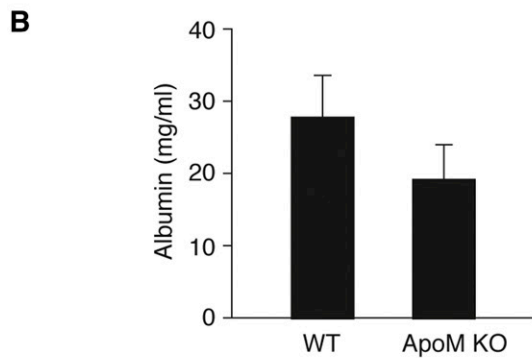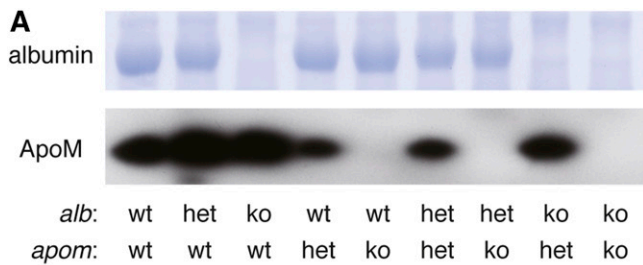
A

albumin

ApoM

| *alb*: | wt | het | ko | wt | wt | het | het | ko | ko |
| *apom*: | wt | wt | wt | het | ko | het | ko | het | ko |

B

C

Fig. 2. Albumin and ApoM protein expression level in the mouse plasma. (A) Plasma (1 μl) from each genotype of the mice was separated by SDS-PAGE. Albumin was revealed by Coomassie Brilliant Blue staining, and ApoM was detected by Western blot analysis by using anti-ApoM antibody (Abcam, #EPR2904). B: Plasma concentration of albumin in WT and ApoM-KO mice was determined using LBIS™ Albumin Mouse ELISA kit (FUJIFILM Wako Pure Chemical Corp.) according to the manufacturer's instructions. Data represent mean ± SD (n = 3). C: Plasma expression level of ApoM in WT and Alb-KO was assessed by Western blot analysis. The intensity of each band was quantified by using ImageJ software (National Institutes of Health). Data represent mean ± SD (n = 3; *$P < 0.01$, by Student's t-test). The figure shows representative data from two independent experiments with basically the same results.

unknown protein(s) serves as S1P chaperones to maintain essential S1P functions.

To identify the S1P-binding protein(s) in the DKO plasma, we pooled S1P-containing LPFP fractions in the DKO sample, and further fractionated by ion-exchange
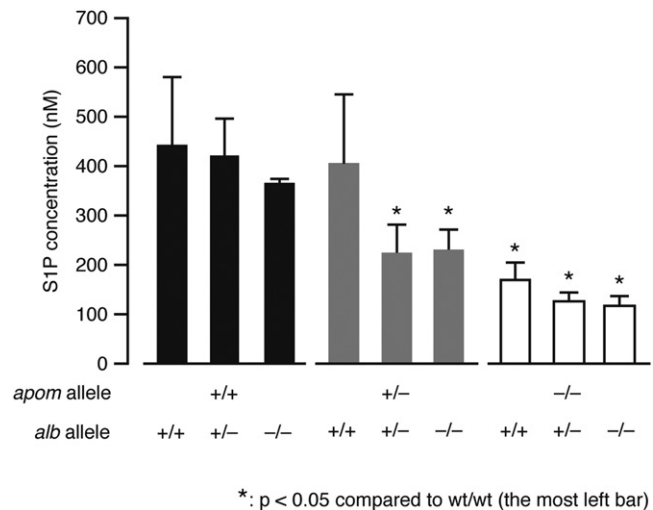

*: $p < 0.05$ compared to wt/wt (the most left bar)

Fig. 3. Total S1P concentrations in the mouse plasma. Plasma samples were collected from each genotype of mice and the S1P concentrations were determined by LC-MS/MS analysis (mean ± SD, n = 4). One-way ANOVA was performed, followed by the post hoc Tukey-Kramer's multiple comparison test (*$P < 0.05$).

chromatography. As shown in **Fig. 5A**, S1P coeluted with the second most prominent protein peak. Out of 746 pmol of S1P in the input sample for the ion-exchange chromatography, 73.8 pmol of S1P was recovered in these fractions. The rest of the S1P was probably absorbed by the column (plastic and/or resin) and was not detected in the eluate. These S1P-containing fractions were pooled together and applied to SDS-PAGE, then visualized by Coomassie Brilliant Blue staining, which revealed the presence of several distinct protein bands (Fig. 5B). The polyacrylamide gel was excised into 12 pieces and digested by trypsin and Lys-C followed by extraction of the peptides, and the peptides were analyzed by a nano-LC-MS/MS system. Identified proteins from the excised bands are shown in supplemental Table S1. Among the proteins listed, we chose AFM, DBP, and ApoA4 for further analysis as potential S1P chaperones (Fig. 5B). This is because AFM, DBP, and aFP are members of the albumin superfamily of plasma proteins, whereas ApoA4 is a known lipid-binding protein. Multiple peptides were identified from ApoA4 in the LC-MS/MS analysis of band 11 (Fig. 5C), suggesting that it coelutes with S1P in the plasma fractions.

We prepared purified recombinant proteins of AFM, DBP, and ApoA4 to examine their S1P-binding properties in vitro (supplemental Fig. S2). Although aFP was not detected in the proteomic analysis, it was also included in the further analysis as a control because it belongs to the albumin superfamily. ApoM and albumin were also prepared under similar conditions. S1P binding assays showed that ApoA4 had significant S1P-binding compared with AFM, DBP, and aFP at the same concentration (**Fig. 6A**). While ApoM showed by far the highest S1P-binding capacity, ApoA4 showed a dose-dependent increase in S1P-binding, which is consistently higher than albumin (Fig. 6B, supplemental Fig. S3).
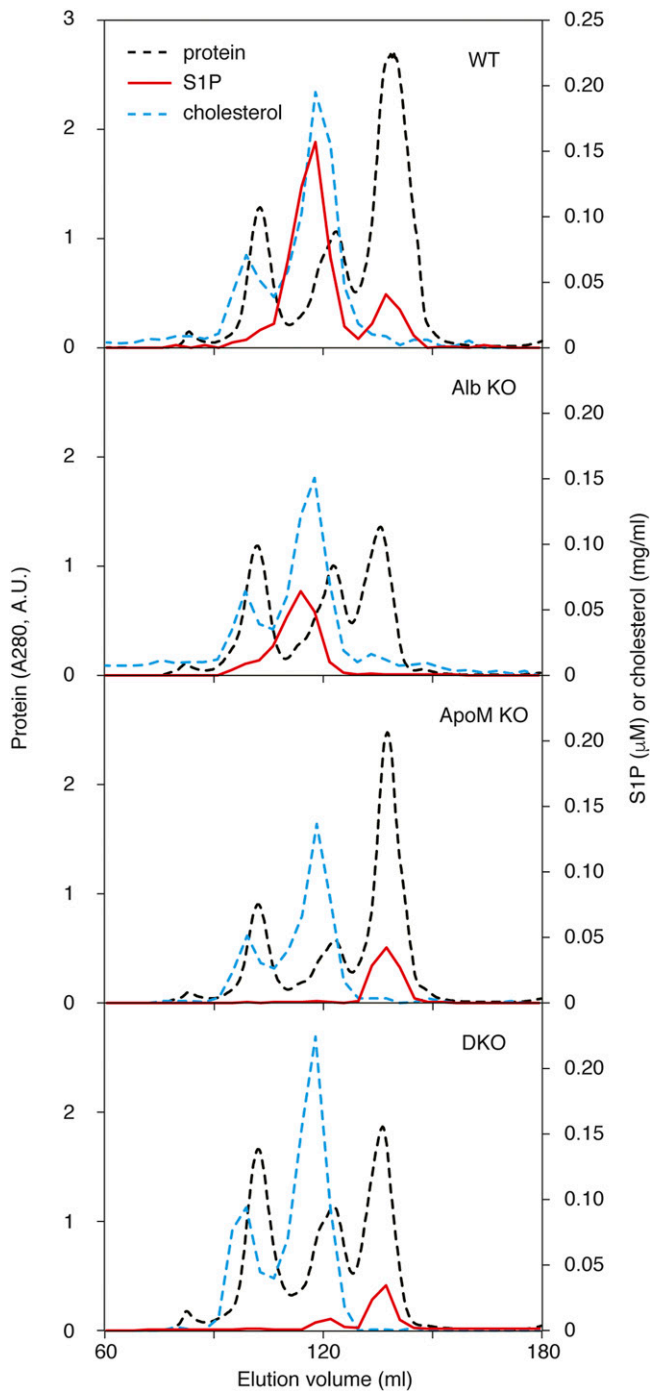
Fig. 4. S1P distribution in lipoprotein and LPFP fractions of mouse plasma. Plasma samples from WT, Alb KO, ApoM KO, and DKO (1 ml each) were separated by size exclusion chromatography with tandemly connected Superose™ 6 and Superdex™ 200 columns (16 × 600 mm each). Absorbance at 280 nm was monitored for protein concentrations (dashed black line). Cholesterol (dashed blue line) and S1P (red line) were determined as described in the Materials and Methods. The figure shows representative data from two independent experiments with basically the same results.

We next checked the ApoA4 distribution in human and mouse plasma. In human plasma, ApoA4 was found mostly in LPFP fractions, and some ApoA4 was associated with the HDL fractions (supplemental Fig. S4A). In the DKO plasma, the ApoA4 elution profile almost completely matched with the S1P distribution, which strongly suggests that ApoA4 serves as a physiological S1P carrier protein, at least in the absence of ApoM and albumin (supplemental Fig. S4B, C). The ApoA4 protein level did not show significant changes depending on the expression of ApoM or albumin (supplemental Fig. S4D, E).

We also examined whether ApoA4-bound S1P can activate S1P receptors. CHO cells expressing either S1P1, S1P2, or S1P3 were stimulated with ApoM, albumin, or ApoA4 containing 100 nM of S1P. ApoA4-bound S1P evoked the activation of Akt and ERK1/2 in S1P1- and S1P3-expressing cells, and the activation of only ERK1/2 in S1P2-expressing cells to the same extent as ApoM- and albumin-bound S1P (**Fig. 7A**, supplemental Fig. S5A). Dose-response studies (Fig. 7B, supplemental Fig. S5B) indicated that nanomolar concentrations of ApoA4-bound S1P stimulated S1P1 and activated ERK1/2.

Human endothelial cells stimulated with either ApoM, albumin, or ApoA4 complexed with S1P showed strong barrier increase (Fig. 7C), whereas these proteins were not effective in the absence of S1P. These data suggest that ApoA4 serves as a S1P chaperone to support critical S1P functions.

DISCUSSION

S1P in circulation is indispensable for embryonic vascular development, vascular barrier integrity, and lymphocyte trafficking (1). Loss of S1P production by sphingosine kinase 1/2 deletion leads to embryonic lethality due to defects in vascular development (19). Adult plasma S1P-less mice show an increase in vascular permeability and profound lymphopenia (2, 23). Also, S1P receptor S1P1 deficiency results in embryonic lethality with almost the same phenotypes as sphingosine kinase 1/2 deletion (24). The S1P chaperone system has evolved to enable efficient transport of S1P in circulation and delivery to the receptors to mediate these essential extracellular S1P functions. We have identified HDL-bound ApoM as a specific and physiologically relevant S1P chaperone (8). ApoM-deficient mice show various functional defects, such as increased vascular permeability (10), exaggerated inflammatory responses (14), and dysregulated lymphopoiesis (11); yet the mice do not show such severe phenotypes as the embryonic lethality observed in sphingosine kinase 1/2 or S1P1 deficiency. This is because 40% of S1P is still retained in circulation carried by another S1P-binding protein, albumin. Albumin is not a specific S1P chaperone and carries various hydrophobic molecules in a promiscuous manner, but still compensates for the functions of ApoM, at least in part.

In this study, we established the mouse line in which these two major S1P carrier proteins are deleted, and found that the mice are still viable and fertile with ~27% S1P retained in circulation. DKO mice did not exhibit discernible abnormalities in behavior and appeared healthy. They showed smaller body size and increased lymphocytes, which were already observed in ApoM-single deficient mice (11, 15). Interestingly, albumin deficiency alone had almost
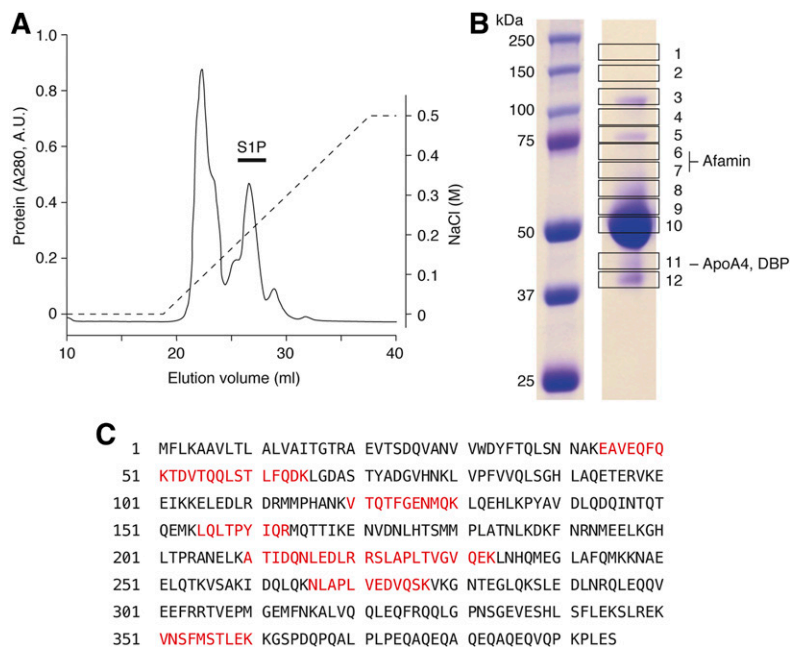
Fig. 5. Purification of S1P-containing protein fractions by ion-exchange chromatography. A: S1P-containing LPFP fractions in the DKO sample from Fig. 4 were pooled and subjected to ion-exchange chromatography with a RESOURCE Q column. A linear gradient of NaCl from 0 to 500 mM (dashed line) was applied to elute the proteins. The figure shows representative data from three independent experiments with basically the same results. B: S1P-containing fractions (black bar in A) were pooled and separated by SDS-PAGE. The gel was cut into 12 pieces as shown and subjected to proteomic analysis by nano LC-MS/MS. AFM was found in bands 6 and 7, and ApoA4 and DBP were found in band 11. C: The peptide sequence of ApoA4 is shown. The peptides detected in the proteomic analysis are highlighted in red.

no effect on the concentration of plasma S1P (Fig. 3), though albumin usually contributes to carrying around 30% of S1P in plasma (7). This is partly explained by the upregulation of ApoM (Fig. 2C). Even in the absence of ApoM, further deletion of albumin only induced a marginal decrease of S1P. These results strongly suggested that additional unknown S1P chaperones function in the absence of ApoM and albumin.

In DKO mice, most of the remaining S1P was found in the LPFP fractions (Fig. 4). We pooled these fractions, further fractionated by ion-exchange chromatography, and identified the putative S1P binding proteins by shot-gun proteomic analysis. From around 30 proteins identified (supplemental Table S1), we picked AFM, DBP, and ApoA4 for further analysis as potential candidates as S1P-binding proteins. Albumin, AFM, and DBP as well as aFP are members of the albumin superfamily of plasma proteins. In humans, all of the genes for the four albumin family proteins are located in chromosome 4 and considered to be generated by gene duplication (25). They have structural similarity, containing three globular domains stabilized by Cys-Cys bonds, which implies that AFM and DBP could accommodate S1P as well, though the concentrations in plasma are much lower than albumin ($\sim$1 μM for AFM and $\sim$5 μM for DBP, compared with $\sim$0.6 mM for albumin). On the other hand, ApoA4 is mainly produced in the small intestine and is associated with chylomicrons in enterocytes (26–28). ApoA4 in circulation is found largely in the lipoprotein-free fraction, whereas a minor fraction is HDL associated. Involvement of ApoA4 in fat absorption and food intake is suggested, but the function of ApoA4 has not been clearly elucidated (29).

We performed in vitro S1P binding assays with these candidate proteins, and only ApoA4 showed a S1P-binding property comparable to albumin (Fig. 6). ApoA4-bound S1P retained the ability to activate S1P1–3 and evoked intracellular signaling events, such as ERK1/2 and Akt activation with nanomolar concentrations of S1P. In vascular endothelial cells, ApoA4-S1P promoted vascular barrier function to the same extent as ApoM- or albumin-S1P. ApoM-S1P showed a prolonged increase in the barrier function compared with albumin-S1P, as reported previously (17), and ApoA4-S1P showed the similar time course as albumin-S1P. These results strongly support the idea that ApoA4 serves as a S1P chaperone to maintain critical S1P functions in the absence of ApoM and albumin.

ApoA4 is a 46 kDa glycoprotein that has structural similarity to the related protein ApoA1 (26, 30). ApoA4 consists of 12 amphipathic helices that enable both hydrophobic and hydrophilic interactions. According to the crystallography data, the 12 helices are arranged into four helical bundles: a long central bundle of 5 helices flanked by a short helix on one end and two bundles of 3 helices on the other end (31, 32). When ApoA4 is lipoprotein free, it exists primarily as a homodimer with the two molecules aligned in an anti-parallel manner. The bundles of helices interact with each other tightly by hydrophobic interactions and create a central hydrophobic pocket in the center region that could accommodate lipid molecules like S1P. When ApoA4 is associated with chylomicrons or HDL, the central hydrophobic pocket becomes loose so that ApoA4 gets twined around the spherical lipoproteins.

The physiological functions of ApoA4 have not been clearly determined. ApoA4 is expressed in the small intestine and secreted into mesenteric lymph to associate with chylomicrons (26). During hydrolysis of the chylomicron triglycerides in the circulation, most of the ApoA4 dissociates from the chylomicrons. As such, involvement of ApoA4 in triglyceride absorption is implicated probably by facilitating chylomicron formation as a structural scaffold (33, 34), but the mechanism has not been clearly elucidated. Anti-oxidative, anti-inflammatory, and anti-atherogenic properties have been described (35–40), and low ApoA4 plasma concentrations are observed in men with coronary
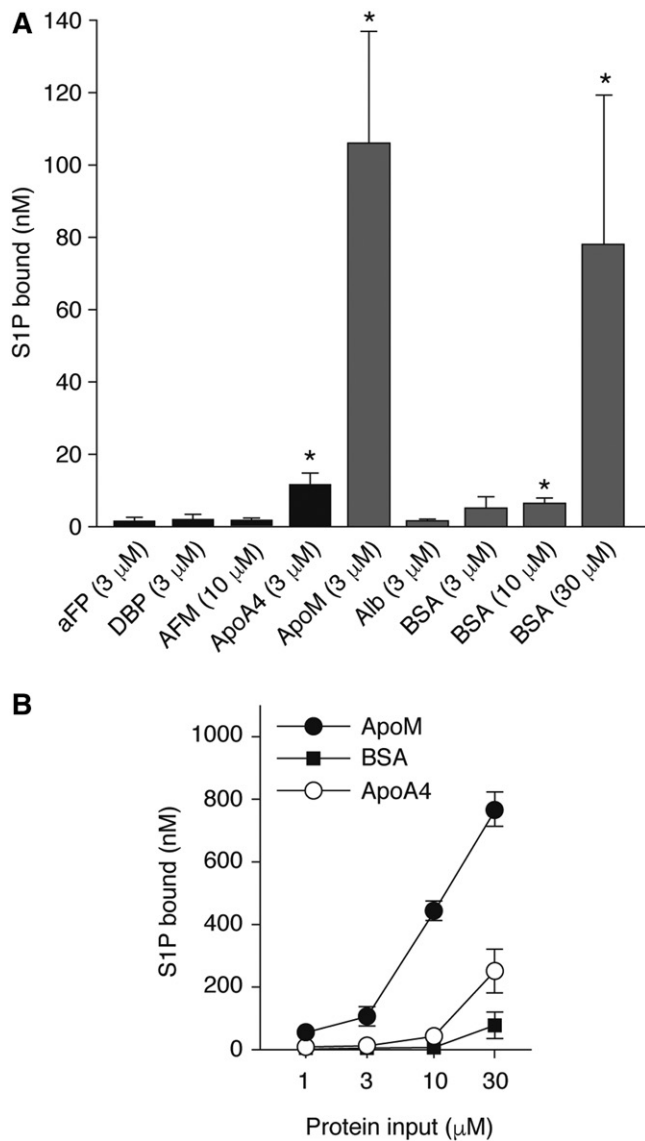
Fig. 6. S1P binding to recombinant ApoA4. S1P (1 μl) was incubated for 24 h at 4°C with one of the recombinant proteins at indicated concentrations (A) or with increasing concentrations of ApoM, ApoA4, or BSA (B). After removing free S1P by desalting columns, the protein-bound S1P was extracted in methanol, and the S1P concentrations were determined by LC-MS/MS analyses. Data represent mean ± SD (n = 3). One-way ANOVA was performed, followed by the post hoc Tukey-Kramer's multiple comparison test (*$P < 0.05$). Close-up comparison between ApoA4 and albumin is shown in supplemental Fig. S3.

Fig. 7. Activation of S1P receptors by ApoA4-bound S1P. A: CHO cells that stably express either S1P1, S1P2, or S1P3 were stimulated with 100 nM of S1P preincubated with the same concentrations of recombinant ApoM, albumin, or ApoA4. After 5 min incubation, total cell lysates were prepared to examine the activation of ERK1/2 and Akt by Western blot analysis. B: CHO cells that stably express S1P1 were stimulated with increasing concentrations of S1P preincubated with recombinant ApoA4. After 5 min incubation, total cell lysates were prepared to examine the activation of ERK1/2 by Western blot analysis. The intensity of each band in A and B was quantified by ImageJ software (National Institutes of Health) and is shown in supplemental Fig. S5. A, B: Data are representative of two independent experiments. C: Confluent HUVECs were cultured on electrode array, and permeability was measured over time via electric cell-substrate impedance sensing instrument. The arrow indicates the time when HUVECs were stimulated with 100 nM albumin (Alb; brown), recombinant ApoM (green), recombinant ApoA4 (purple), or the proteins preincubated with the same concentration of S1P (Alb-S1P, red; ApoM-S1P, orange; ApoA4-S1P, blue). The data represent mean ± SD and are representative of at least three experiments.

artery disease (41). ApoA4 is also involved in glucose metabolism and insulin secretion from pancreatic β-cells. Exogenous ApoA4 stimulates insulin secretion in a dose-dependent manner in vitro, and ApoA4 KO mice fed a chow diet are glucose intolerant due to attenuated insulin secretion in response to a glucose challenge (42). A recent study found that ApoA4 is associated with activated platelets via direct binding to the platelet glycoprotein αIIbβ3 integrin and suppresses platelet aggregation. Further, postprandial increase in platelet aggregability is inhibited by plasma ApoA4 (43). Whether this novel function of ApoA4 requires S1P action is not known. Because ApoM-bound
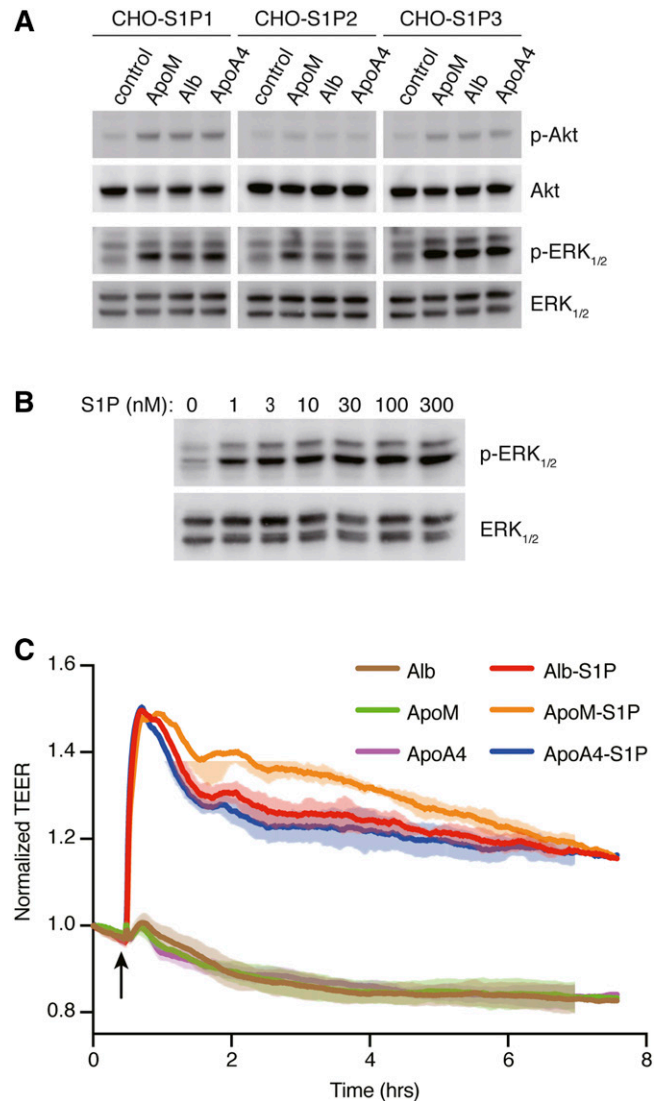
S1P also exhibits anti-inflammatory and anti-atherogenic properties (14) as well as regulatory functions of glucose/fat metabolism (15, 44), it is possible that some of the proposed functions of ApoA4 might be exerted by its cargo S1P.

The limitation of this study is that the physiological relevance of ApoA4 as a S1P carrier has not been firmly established. Although ApoA4 serves as a S1P chaperone to maintain essential extracellular S1P function in the absence of both ApoM and albumin, the double-deficient condition was created by the gene manipulations and is artificial. We performed immunoprecipitation of ApoA4 in human plasma but did not detect S1P in the precipitates (data not shown), suggesting that ApoA4 does not carry S1P in the physiological plasma in which ApoM and albumin exist abundantly. However, we cannot exclude the possibility that ApoA4 binding to S1P may be antagonized by anti-ApoA4 antibody binding, resulting in no S1P detection in the anti-ApoA4 immune complexes. ApoA4 is also found in mesenteric lymph and cerebrospinal fluid (45), where ApoM or albumin concentrations are usually low. ApoA4 might have some specific functions as a S1P chaperone in the environment where other S1P chaperones are not available. In the future, it would be useful to analyze S1P concentrations in various tissues in ApoA4-deficient mice or in ApoM/albumin/ApoA4 triple-deficient mice.

In summary, we describe ApoA4 as a novel S1P chaperone that can maintain essential extracellular S1P functions in the absence of ApoM and albumin. Our data suggest that multiple S1P chaperone systems have evolved to support indispensable S1P functions in circulation in a redundant manner.

REFERENCES

1. Yanagida, K., and T. Hla. 2017. Vascular and immunobiology of the circulatory sphingosine 1-phosphate gradient. *Annu. Rev. Physiol.* **79:** 67–91.

2. Pappu, R., S. R. Schwab, I. Cornelissen, J. P. Pereira, J. B. Regard, Y. Xu, E. Camerer, Y. W. Zheng, Y. Huang, J. G. Cyster, et al. 2007. Promotion of lymphocyte egress into blood and lymph by distinct sources of sphingosine-1-phosphate. *Science.* **316:** 295–298.

3. Venkataraman, K., Y. M. Lee, J. Michaud, S. Thangada, Y. Ai, H. L. Bonkovsky, N. S. Parikh, C. Habrukowich, and T. Hla. 2008. Vascular endothelium as a contributor of plasma sphingosine 1-phosphate. *Circ. Res.* **102:** 669–676.

4. Vu, T. M., A. N. Ishizu, J. C. Foo, X. R. Toh, F. Zhang, D. M. Whee, F. Torta, A. Cazenave-Gassiot, T. Matsumura, S. Kim, et al. 2017. Mfsd2b is essential for the sphingosine-1-phosphate export in erythrocytes and platelets. *Nature.* **550:** 524–528.

5. Kawahara, A., T. Nishi, Y. Hisano, H. Fukui, A. Yamaguchi, and N. Mochizuki. 2009. The sphingolipid transporter spns2 functions in migration of zebrafish myocardial precursors. *Science.* **323:** 524–527.

6. Fukuhara, S., S. Simmons, S. Kawamura, A. Inoue, Y. Orba, T. Tokudome, Y. Sunden, Y. Arai, K. Moriwaki, J. Ishida, et al. 2012. The sphingosine-1-phosphate transporter Spns2 expressed on endothelial cells regulates lymphocyte trafficking in mice. *J. Clin. Invest.* **122:** 1416–1426.

7. Murata, N., K. Sato, J. Kon, H. Tomura, M. Yanagita, A. Kuwabara, M. Ui, and F. Okajima. 2000. Interaction of sphingosine 1-phosphate with plasma components, including lipoproteins, regulates the lipid receptor-mediated actions. *Biochem. J.* **352:** 809–815.

8. Christoffersen, C., H. Obinata, S. B. Kumaraswamy, S. Galvani, J. Ahnström, M. Sevvana, C. Egerer-Sieber, Y. A. Muller, T. Hla, L. B. Nielsen, et al. 2011. Endothelium-protective sphingosine-1-phosphate provided by HDL-associated apolipoprotein M. *Proc. Natl. Acad. Sci. USA.* **108:** 9613–9618.

9. Christoffersen, C., J. Ahnström, O. Axler, E. I. Christensen, B. Dahlbäck, and L. B. Nielsen. 2008. The signal peptide anchors apolipoprotein M in plasma lipoproteins and prevents rapid clearance of apolipoprotein M from plasma. *J. Biol. Chem.* **283:** 18765–18772.

10. Christensen, P. M., C. H. Liu, S. L. Swendeman, H. Obinata, K. Qvortrup, L. B. Nielsen, T. Hla, A. Di Lorenzo, and C. Christoffersen. 2016. Impaired endothelial barrier function in apolipoprotein M-deficient mice is dependent on sphingosine-1-phosphate receptor 1. *FASEB J.* **30:** 2351–2359.

11. Blaho, V. A., S. Galvani, E. Engelbrecht, C. Liu, S. L. Swendeman, M. Kono, R. L. Proia, L. Steinman, M. H. Han, and T. Hla. 2015. HDL-bound sphingosine-1-phosphate restrains lymphopoiesis and neuroinflammation. *Nature.* **523:** 342–346.

12. Kurano, M., K. Tsukamoto, R. Ohkawa, M. Hara, J. Iino, Y. Kageyama, H. Ikeda, and Y. Yatomi. 2013. Liver involvement in sphingosine 1-phosphate dynamism revealed by adenoviral hepatic overexpression of apolipoprotein M. *Atherosclerosis.* **229:** 102–109.

13. Ding, B. S., C. H. Liu, Y. Sun, Y. Chen, S. L. Swendeman, B. Jung, D. Chavez, Z. Cao, C. Christoffersen, L. B. Nielsen, et al. 2016. HDL activation of endothelial sphingosine-1-phosphate receptor-1 (S1P1) promotes regeneration and suppresses fibrosis in the liver. *JCI Insight.* **1:** e87058.

14. Galvani, S., M. Sanson, V. A. Blaho, S. L. Swendeman, H. Obinata, H. Conger, B. Dahlbäck, M. Kono, R. L. Proia, J. D. Smith, et al. 2015. HDL-bound sphingosine 1-phosphate acts as a biased agonist for the endothelial cell receptor S1P1 to limit vascular inflammation. *Sci. Signal.* **8:** ra79. [Erratum. 2015. *Sci. Signal.* 8: er8.]

15. Christoffersen, C., C. K. Federspiel, A. Borup, P. M. Christensen, A. N. Madsen, M. Heine, C. H. Nielsen, A. Kjaer, B. Holst, J. Heeren, et al. 2018. The apolipoprotein M/S1P axis controls triglyceride metabolism and brown fat activity. *Cell Reports.* **22:** 175–188.

16. Swendeman, S. L., Y. Xiong, A. Cantalupo, H. Yuan, N. Burg, Y. Hisano, A. Cartier, C. H. Liu, E. Engelbrecht, V. Blaho, et al. 2017. An engineered S1P chaperone attenuates hypertension and ischemic injury. *Sci. Signal.* **10:** eaal2722.

17. Wilkerson, B. A., G. D. Grass, S. B. Wing, W. S. Argraves, and K. M. Argraves. 2012. Sphingosine 1-phosphate (S1P) carrier-dependent regulation of endothelial barrier: high density lipoprotein (HDL)-S1P prolongs endothelial barrier enhancement as compared with albumin-S1P via effects on levels, trafficking, and signaling of S1P1. *J. Biol. Chem.* **287:** 44645–44653.

18. Kimura, T., K. Sato, A. Kuwabara, H. Tomura, M. Ishiwara, I. Kobayashi, M. Ui, and F. Okajima. 2001. Sphingosine 1-phosphate may be a major component of plasma lipoproteins responsible for the cytoprotective actions in human umbilical vein endothelial cells. *J. Biol. Chem.* **276:** 31780–31785.

19. Mizugishi, K., T. Yamashita, A. Olivera, G. F. Miller, S. Spiegel, and R. L. Proia. 2005. Essential role for sphingosine kinases in neural and vascular development. *Mol. Cell. Biol.* **25:** 11113–11121.

20. Christoffersen, C., M. Jauhiainen, M. Moser, B. Porse, C. Ehnholm, M. Boesl, B. Dahlbäck, and L. B. Nielsen. 2008. Effect of apolipoprotein M on high density lipoprotein metabolism and atherosclerosis in low density lipoprotein receptor knock-out mice. *J. Biol. Chem.* **283:** 1839–1847.

21. Frej, C., A. Andersson, B. Larsson, L. J. Guo, E. Norström, K. E. Happonen, and B. Dahlbäck. 2015. Quantification of sphingosine 1-phosphate by validated LC-MS/MS method revealing strong correlation with apolipoprotein M in plasma but not in serum due to platelet activation during blood coagulation. *Anal. Bioanal. Chem.* **407:** 8533–8542.

22. Aso, C., M. Araki, N. Ohshima, K. Tatei, T. Hirano, H. Obinata, M. Kishi, K. Kishimoto, A. Konishi, F. Goto, et al. 2016. Protein purification and cloning of diacylglycerol lipase from rat brain. *J. Biochem.* **159:** 585–597.

23. Camerer, E., J. B. Regard, I. Cornelissen, Y. Srinivasan, D. N. Duong, D. Palmer, T. H. Pham, J. S. Wong, R. Pappu, and S. R. Coughlin. 2009. Sphingosine-1-phosphate in the plasma compartment regulates basal and inflammation-induced vascular leak in mice. *J. Clin. Invest.* **119:** 1871–1879.

24. Liu, Y., R. Wada, T. Yamashita, Y. Mi, C. X. Deng, J. P. Hobson, H. M. Rosenfeldt, V. E. Nava, S. S. Chae, M. J. Lee, et al. 2000. Edg-1, the G protein-coupled receptor for sphingosine-1-phosphate, is essential for vascular maturation. *J. Clin. Invest.* **106:** 951–961.

25. Lichenstein, H. S., D. E. Lyons, M. M. Wurfel, D. A. Johnson, M. D. McGinley, J. C. Leidli, D. B. Trollinger, J. P. Mayer, S. D. Wright, and M. M. Zukowski. 1994. Afamin is a new member of the albumin,

alpha-fetoprotein, and vitamin D-binding protein gene family. *J. Biol. Chem.* **269:** 18149–18154.

26. Utermann, G., and U. Beisiegel. 1979. Apolipoprotein A-IV: a protein occurring in human mesenteric lymph chylomicrons and free in plasma. Isolation and quantification. *Eur. J. Biochem.* **99:** 333–343.

27. Karathanasis, S. K., I. Yunis, and V. I. Zannis. 1986. Structure, evolution, and tissue-specific synthesis of human apolipoprotein AIV. *Biochemistry.* **25:** 3962–3970.

28. Staels, B., A. van Tol, G. Verhoeven, and J. Auwerx. 1990. Apolipoprotein A-IV messenger ribonucleic acid abundance is regulated in a tissue-specific manner. *Endocrinology.* **126:** 2153–2163.

29. Wang, F., A. B. Kohan, C. M. Lo, M. Liu, P. Howles, and P. Tso. 2015. Apolipoprotein A-IV: a protein intimately involved in metabolism. *J. Lipid Res.* **56:** 1403–1418.

30. Karathanasis, S. K. 1985. Apolipoprotein multigene family: tandem organization of human apolipoprotein AI, CIII, and AIV genes. *Proc. Natl. Acad. Sci. USA.* **82:** 6374–6378.

31. Deng, X., J. Morris, J. Dressmen, M. R. Tubb, P. Tso, W. G. Jerome, W. S. Davidson, and T. B. Thompson. 2012. The structure of dimeric apolipoprotein A-IV and its mechanism of self-association. *Structure.* **20:** 767–779.

32. Deng, X., J. Morris, C. Chaton, G. F. Schröder, W. S. Davidson, and T. B. Thompson. 2013. Small-angle X-ray scattering of apolipoprotein A-IV reveals the importance of its termini for structural stability. *J. Biol. Chem.* **288:** 4854–4866.

33. Hayashi, H., D. F. Nutting, K. Fujimoto, J. A. Cardelli, D. Black, and P. Tso. 1990. Transport of lipid and apolipoproteins A-I and A-IV in intestinal lymph of the rat. *J. Lipid Res.* **31:** 1613–1625.

34. Lu, S., Y. Yao, X. Cheng, S. Mitchell, S. Leng, S. Meng, J. W. Gallagher, G. S. Shelness, G. S. Morris, J. Mahan, et al. 2006. Overexpression of apolipoprotein A-IV enhances lipid secretion in IPEC-1 cells by increasing chylomicron size. *J. Biol. Chem.* **281:** 3473–3483.

35. Stein, O., Y. Stein, M. Lefevre, and P. S. Roheim. 1986. The role of apolipoprotein A-IV in reverse cholesterol transport studied with cultured cells and liposomes derived from an ether analog of phosphatidylcholine. *Biochim. Biophys. Acta.* **878:** 7–13.

36. Qin, X., D. K. Swertfeger, S. Zheng, D. Y. Hui, and P. Tso. 1998. Apolipoprotein AIV: a potent endogenous inhibitor of lipid oxidation. *Am. J. Physiol.* **274:** H1836–H1840.

37. von Eckardstein, A., Y. Huang, S. Wu, A. S. Sarmadi, S. Schwarz, A. Steinmetz, and G. Assmann. 1995. Lipoproteins containing apolipoprotein A-IV but not apolipoprotein A-I take up and esterify cell-derived cholesterol in plasma. *Arterioscler. Thromb. Vasc. Biol.* **15:** 1755–1763.

38. Fournier, N., V. Atger, J. L. Paul, M. Sturm, N. Duverger, G. H. Rothblat, and N. Moatti. 2000. Human ApoA-IV overexpression in transgenic mice induces cAMP-stimulated cholesterol efflux from J774 macrophages to whole serum. *Arterioscler. Thromb. Vasc. Biol.* **20:** 1283–1292.

39. Ostos, M. A., M. Conconi, L. Vergnes, N. Baroukh, J. Ribalta, J. Girona, J. M. Caillaud, A. Ochoa, and M. M. Zakin. 2001. Antioxidative and antiatherosclerotic effects of human apolipoprotein A-IV in apolipoprotein E-deficient mice. *Arterioscler. Thromb. Vasc. Biol.* **21:** 1023–1028.

40. Vowinkel, T., M. Mori, C. F. Krieglstein, J. Russell, F. Saijo, S. Bharwani, R. H. Turnage, W. S. Davidson, P. Tso, D. N. Granger, et al. 2004. Apolipoprotein A-IV inhibits experimental colitis. *J. Clin. Invest.* **114:** 260–269.

41. Kronenberg, F., M. Stühlinger, E. Trenkwalder, F. S. Geethanjali, O. Pachinger, A. von Eckardstein, and H. Dieplinger. 2000. Low apolipoprotein A-IV plasma concentrations in men with coronary artery disease. *J. Am. Coll. Cardiol.* **36:** 751–757.

42. Wang, F., A. B. Kohan, T. L. Kindel, K. L. Corbin, C. S. Nunemaker, S. Obici, S. C. Woods, W. S. Davidson, and P. Tso. 2012. Apolipoprotein A-IV improves glucose homeostasis by enhancing insulin secretion. *Proc. Natl. Acad. Sci. USA.* **109:** 9641–9646.

43. Xu, X. R., Y. Wang, R. Adili, L. Ju, C. M. Spring, J. W. Jin, H. Yang, M. A. D. Neves, P. Chen, Y. Yang, et al. 2018. Apolipoprotein A-IV binds αIIbβ3 integrin and inhibits thrombosis. *Nat. Commun.* **9:** 3608.

44. Kurano, M., M. Hara, K. Tsuneyama, H. Sakoda, T. Shimizu, K. Tsukamoto, H. Ikeda, and Y. Yatomi. 2014. Induction of insulin secretion by apolipoprotein M, a carrier for sphingosine 1-phosphate. *Biochim. Biophys. Acta.* **1841:** 1217–1226.

45. Borghini, I., F. Barja, D. Pometta, and R. W. James. 1995. Characterization of subpopulations of lipoprotein particles isolated from human cerebrospinal fluid. *Biochim. Biophys. Acta.* **1255:** 192–200.